**ISCI, Volume *19***

## Supplemental Information

# The Input-Output Relationship of AIY Interneurons in *Caenorhabditis elegans* in Noisy Environment

**Keita Ashida, Kohji Hotta, and Kotaro Oka**

# Supplemental Information
# Transparent methods
## *C. elegans* strains

Worms were cultured at 20°C on nematode growth medium agar plates with *Escherichia coli* OP50 bacteria under standard conditions (Brenner, 1974). Hermaphrodites were used for all experiments. The following transgenic strains were created via microinjection into the Bristol strain N2 (wild type), RB594 *glc-3* (ok321) V, and MT6308 *eat-4* (ky5) III. The transgenic strains used for this research were as follows: *okaEx5[pttx-3::iGluSnFR, 50 ng/μL + pttx-3::R-GECO1, 50 ng/μL]*, *okaEx6[pttx-3::ArcLight, 50 ng/μL + pttx-3::R-GECO1, 50 ng/μL]*, *okaEx10[pttx-3::GCaMP6, 50 ng/μL + pttx-3::dimer2, 50 ng/μL], okaEx15; glc-3 (ok321) X [pttx-3::iGluSnFR, 50 ng/μL + pttx-3::R-GECO1, 40 ng/μL + punc-122::dsRed, 15 ng/μL]*, and *okaEx16; eat-4 (ky5) X [pttx-3::iGluSnFR, 50 ng/μL + pttx-3::R-GECO1, 40 ng/μL + punc-122::dsRed 15 ng/μL]*.

## Plasmids

For ArcLight expression, codon-optimized ArcLight was synthesized using *C. elegans* Codon Adapter (Redemann et al., 2011) (Integrated DNA Technologies Genes). This codon-optimized ArcLight was cloned into a Gateway Destination vector (Thermo Fisher Scientific). Gateway Destination vectors for expressing proteins and Gateway Entry vectors (Thermo Fisher Scientific) for cell-specific promoters were obtained from the Comprehensive Brain Science Network. All plasmids used to express proteins in the animals were generated from these vectors using Gateway Cloning Technology (Thermo Fisher Scientific).

## Confocal imaging

Confocal images of detailed neuronal structures (Figures 1A and 2A) were acquired using a confocal laser scanning microscopy system (FluoView FV1000, Olympus) mounted on an inverted microscope (IX81, Olympus) using a 40× objective oil-immersion lens (UPLFLN 40XO, Olympus) for animals expressing ArcLight and R-GECO or iGluSnFR and R-GECO in their AIY neurons. Animals were immobilized with 20 mM sodium azide and mounted in a 1% low-melting-point agarose gel (UltraPure, Invitrogen). The imaging conditions were excitation at 488 nm and detection at 500–545 nm for ArcLight and iGluSnFR, and excitation at 559 nm and detection at 570–670 nm for R-GECO.

## $Ca^{2+}$, glutamate and voltage imaging

We used a genetically encoded $Ca^{2+}$ indicator, R-GECO1 (Zhao et al., 2011), a genetically encoded $Ca^{2+}$ indicator, G-CaMP6 (Ohkura et al., 2012) with dimer 2 (Campbell et al., 2002) (RFP as a reference), a genetically encoded glutamate indicator, iGluSnFR (Marvin et al., 2013), and a genetically encoded voltage indicator, ArcLight (Jin et al., 2012) with olfactory chips (Chronis et al., 2007). The olfactory chips are microfluidic devices that can control stimulation temporally via valve switching. The animals were stimulated with S-basal buffer and isoamyl alcohol (IAA) diluted with S-basal buffer ($9.2 \times 10^{-4}$ mol/L). For $Ca^{2+}$ and glutamate imaging, the animals were stimulated with 60 s S-basal buffer, 60 s diluted IAA, and again 60 s S-basal buffer (as shown in Figure 3B). To simultaneously image $Ca^{2+}$ and membrane potential under odor stimulation, images were acquired over 70 s immediately after switching from S-basal to diluted IAA. For the no-odor condition, images were acquired without changing the buffer. To reduce the effects of photobleaching, we used images taken after 60 s for analysis. Images were acquired every 100 ms for $Ca^{2+}$ and glutamate imaging, and every 20 ms for $Ca^{2+}$ and membrane potential imaging; the exposure time was equal to the interval duration (100 or 20 ms) in each case. We used an inverted microscope (IX71, Olympus) with a LED light source (SOLA, Lumencor), and a 3CCD camera (C7800-20, Hamamatsu Photonics). Images were acquired using an AQUACOSMOS (Hamamatsu Photonics) with a 20× objective lens (UCPLFLN 20X, Olympus) and a 1.6× zoom lens. A BrightLine GFP/DSRED-A (Semrock) cube was used. We noted that ArcLight becomes dim when the membrane potential depolarizes, while R-GECO becomes bright when $Ca^{2+}$ increases. The membrane potential spikes in Figures 1B and 1C are thus not artifacts of fluorescent leakage by R-GECO. In addition, photobleaching causes an increase of the ArcLight traces in Figure 1B because we showed $-\Delta F/F_0$ for the ArcLight traces. To reduce noise caused by movement of the animals, a cholinergic agonist, levamisole (2 mM), was used in the S-basal buffer. In preliminary experiments, we demonstrated that levamisole did not affect the AIY spike frequency (Figure S1).

## Image analysis

We analyzed the imaging data using the same semi-automated custom software written in MATLAB (MathWorks) that we used in a previous study (Shidara et al., 2017). Regions

of interest were determined based on fluorescence intensities and the morphology of the neurons (Figures 1A and 2A). We measured the $Ca^{2+}$ response and glutamate input at the AIY neurite, because these interneurons show a clear $Ca^{2+}$ response at the neurite but not at the soma (Chalasani et al., 2007; Clark et al., 2006). All fluorescence intensity data were normalized by the average intensities for the first 2 s, and are presented as ΔF/F.

## Data analysis and statistical tests

Statistical tests were performed in Excel 2011 (paired t-test and Welch's t-test, using the "TTEST" function), Python 3 (version: 3.7.0; tests for Pearson correlation coefficients were conducted using the "stats.pearsonr" function in the SciPy library (version 1.1.0)), and R (version: 3.4.3; Wilcoxon signed rank tests were conducted using the "wilcoxsign_test" function with the "exact" option, and Wilcoxon rank sum tests were conducted using the "wilcox_test" function with the "exact" option in the coin package).

The average intensities of the $Ca^{2+}$ and membrane potential spikes in Figure 1C were generated by detecting $Ca^{2+}$ spikes as described below. The peak values of membrane potential in Figures 1D and 1E were calculated by subtracting the average values for the 1 s period from −1 s to −2 s in Figure 1C from the maximal values for the 1 s period from −1 s to 0 s. The $Ca^{2+}$ increases were calculated by subtracting the average intensities for the 1 s period from −1 s to 0 s from the maximal intensities for the 1 s period from 0.5 s to 1.5 s.

The averaged intensities over the 20 s before and after odor addition are shown in Figure 2C (left), and the average intensities over the 20 s before and after odor removal are shown in Figure 2C (right).

We classified the odor stimulation conditions into two groups, early odor and later odor, for Figures 3–6. The early odor condition comprised the data from the first 10 s after the onset of odor stimulation, and the later odor condition comprised the data from 10–60 s after odor addition (see Figure 3B). Odor addition reduced glutamate-input levels immediately (Figure 2B), so we considered two conditions to be transient and stable, respectively.

We classified the data based on whether $Ca^{2+}$ spikes were present or absent (with or without) for Figures 3, 5, and 6. The $Ca^{2+}$ spikes in Figure 3C were extracted as described below, and data that did not include $Ca^{2+}$ spikes were considered non-$Ca^{2+}$

spiking data. All glutamate responses were normalized to zero at time 0. The intensities before the $Ca^{2+}$ spike ("pre" in Figure 3D) are the average intensities for the 1 s period from −3 s to −2 s in Figure 3C, and the average intensities during the spike ("onset" in Figure 3D) are the average intensities for the 1 s period from −0.5 s to +0.5 s in Figure 3C. The glutamate decreases in Figure 3E and 3F were calculated by subtracting the "onset" intensities in Figure 3D from the "pre" intensities. The $Ca^{2+}$ increases in Figure 3E were calculated by subtracting the average intensities for the 1 s period from −1 s to 0 s (as in Figure 3C) from the average intensities for the 1 s period from 2 s to 3 s.

The $Ca^{2+}$ responses to glutamate decreases, shown in Figure 4A were collected as described below. All $Ca^{2+}$ responses were normalized to zero at time 0. The intensities before and during the response in Figure 4B were calculated as for Figure 3D. The randomly selected data in Figures 4C and 4D are described below. The $Ca^{2+}$ increases shown in Figure 4D were calculated by subtracting the average intensities before the response ("pre" in Figure 4B) from those during the response ("onset" in Figure 4B).

The average intensities of the glutamate input shown in Figure 5B were calculated as for Figure 2C; Figures 5C–5E were generated in the same manner as Figures 3C, 3D, and 3F.

The average intensities of glutamate input shown in Figure 6B were calculated as for Figure 2C. The probability of a $Ca^{2+}$ spike in response to odor stimulation shown in Figure 6C was calculated by counting the $Ca^{2+}$ spikes during the early-odor period. The frequency of the $Ca^{2+}$ spikes in Figure 6D was calculated by counting the $Ca^{2+}$ spikes detected as described below. Figures 6E–6G were generated in the same manner as Figures 3C, 3D, and 3F.

## Extracting $Ca^{2+}$ spikes and glutamate decreases

To extract the $Ca^{2+}$ spikes, we selected a data point at near the beginning of the $Ca^{2+}$ data, and calculated the difference between the average intensities for the 5 s period before and after before that point. If the difference was larger than the average intensity over the 5 s period before the point plus three standard deviations, the point was determined to be the onset of a $Ca^{2+}$ spike, after visual verification. To extract the glutamate-decrease point shown in Figure 4, we selected a data point at near the beginning of the glutamate data and calculated the difference between the averaged intensities for the 5 s period before and after that point. If the difference was larger than the threshold (0.025; determined

from the values in Figure 3F), the point was automatically determined to be the onset of a glutamate decrease. For $Ca^{2+}$ and glutamate decreases, we collected the data for 5 s periods before and after the points that had been detected as described above. There was no overlap between the collected data. Finally, we defined all data that did not include a $Ca^{2+}$ spike as the data without a $Ca^{2+}$ spike.

In Figure S1, we counted the $Ca^{2+}$ spikes manually, because the signal-to-noise ratio differed between the with- and without-levamisole conditions. We counted the spikes from 70 s to 120 s for Figure S1B, and from 60 s to 70 s for Figure S1C.

## Random resampling

Randomly resampled data are used in Figures 4C and 4D. One hundred time points were selected randomly using the "randint" function (in Python numpy.random in NumPy library (version 1.15.2)), and we extracted 10 s of data after each of these points. We initialized the seed of the random number generator using the current system time.

# Supplemental figures

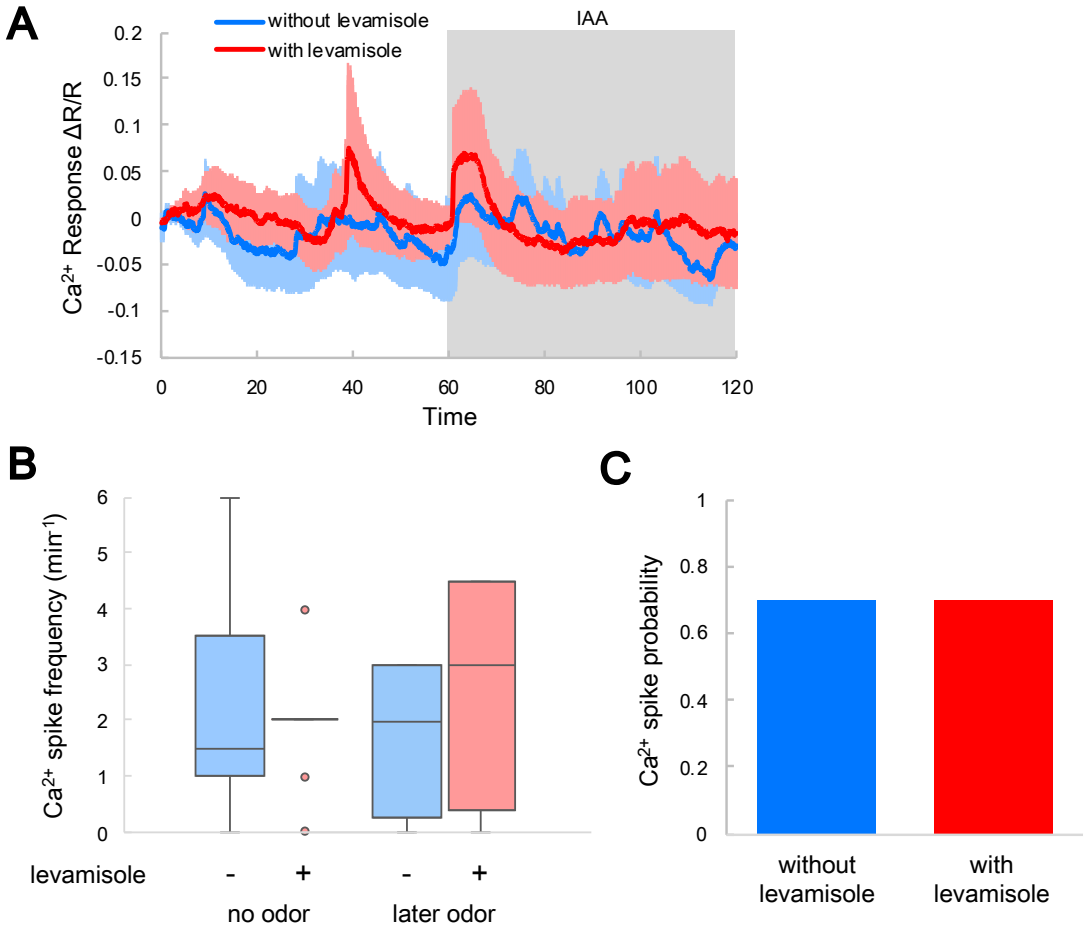


**Figure S1.** Levamisole does not significantly affect $Ca^{2+}$ spikes in AIY. Related to Figure 1.

**(A)** The $Ca^{2+}$ response in AIY to odor with (red) and without (blue) levamisole. The shaded region is odor stimulation.

**(B)** Spike frequency without (from 0 s to 60 s) and with (from 70 s to 120 s) odor stimulation, with (red) and without (blue) levamisole. Box plots indicate the median (center line), quartiles (boxes), and range (whiskers). The statistical metrics are as follows: no odor, p = 0.75, later odor, p = 0.80. Wilcoxon rank sum test (without levamisole, N = 10; with levamisole, N = 10).

**(C)** $Ca^{2+}$ spike probability immediately after odor stimulation with and without levamisole. The statistical metrics are as follows; p = 1.0, Fisher's exact test (without levamisole, N = 10; with levamisole, N = 10).

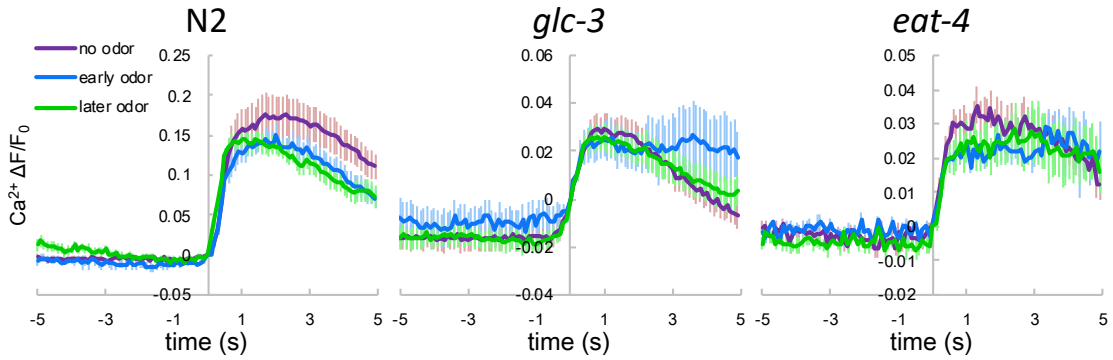


**Figure S2.** Averaged $Ca^{2+}$ responses. Related to Figures 3, 5 and 6.

Time 0 indicates the onset of $Ca^{2+}$ spikes. All $Ca^{2+}$ responses were normalized to zero at time 0. The purple, blue and green lines indicate the responses under the no-odor, early-odor, and later-odor conditions, respectively. Shadows indicate the SEM (N2: N = 15; no odor, n = 15; early odor, n = 11; later odor, n = 20; *glc-3*: N = 12, no odor, n = 15; early odor, n = 6; later odor, n = 20; *eat-4*: N = 12, no odor: n = 9; early odor, n = 3; later odor, n = 9).